

Recent Advances in Partial Discharge Measurement Capabilities at NIST

R. J. Van Brunt, K. L. Stricklett

National Institute of Standards and Technology,
Gaithersburg MD

J. P. Steiner

Biddle Instruments, Blue Bell, PA

and S. V. Kulkarni

Institute for Plasma Research, Bhat, Gandhinagar,
India

ABSTRACT

This report describes three techniques under development at the National Institute of Standards and Technology (NIST) to measure the properties of partial discharges (PD). These measurements are useful in providing new insight into the mechanisms that influence or control PD behavior and in affording a means of locating PD activity in cables. The first is concerned with an advanced, real-time PD measurement system that allows a 'complete' characterization of the stochastic properties of PD. With this system it is possible to measure a set of conditional PD pulse amplitude and pulse-time separation distributions from which memory effects characteristic of the discharge phenomena can be quantified and interpreted. Examples of results obtained for pulsating negative corona discharges in gases are shown. The second technique allows PD location in cables using time-domain reflectometry with appropriate statistical analysis. With the third technique discussed here, simultaneous measurements are made of the optical and electrical characteristics of PD in liquid dielectrics using fast photography combined with broad-band, low-noise pulse current measurements. This method provides a detailed description of the temporal and spatial development of PD in highly nonuniform field configurations. Examples of results are shown for the case of PD in hexanes when a dc voltage is applied to a point-rod electrode gap.

1. INTRODUCTION

PARTIAL-DISCHARGE (PD) measurements have long been recognized as an important part of quality control for HV apparatus. There is also increasing interest in the use of PD measurement as a diagnostic tool for assessing insulation performance and integrity when subjected to electrical and mechanical stress. The measurement of PD has been applied to a wide range of electrical apparatus including rotating machines, power transformers, and both low- and HV cables [1].

The PD phenomenon under consideration here is a self-quenching discharge that is localized in regions of high electrical stress within insulating systems. The high-stress regions might, for example, be associated with voids or 'trees' in solid dielectrics, metal particles or sharp points on either solid conductors or insulators, or the presence of interfaces between different types of insulating or conducting media. PD is self-quenching because surface or space charge produced during the discharge generally accumulates at the discharge site and reduces the magnitude of the local electric-field to a level insufficient to sustain the discharge.

Because of its self-quenching nature, the PD phenomenon is inherently pulsating and will manifest itself as current pulses in the external circuit. PD activity occurs in regions that are at least partially in the gas phase such as occlusions in solids or 'bubbles' formed by vaporization of a liquid. The PD phenomenon that occur around conductors in air or other gases is often referred to as *corona*. It should be noted that corona discharges can, under some conditions, exhibit a non-pulsating characteristic for dc voltages that is associated with the formation of a steady glow region [2,3]. Because this type of corona discharge is steady and therefore not self quenching, it does not fit into the category of PD phenomena under consideration here.

PD can be observed by electrical, optical, or acoustical measurements that detect and record pulses. The determination of PD pulse characteristics has been the subject of numerous investigations [4]. Techniques have been developed to measure such parameters as mean pulse amplitude and repetition rate [5], pulse-height distribution [6-8], pulse shapes [9], correlation of pulse amplitude with phase of an ac voltage [10-12], and correlation between optical, electrical, or acoustical pulses. Because of the complex, stochastic nature of PD phenomena, the results of such measurements have often been difficult, if not impossible, to interpret in terms of meaningful physical models. The measurement schemes discussed here are, in some sense, extensions of techniques previously used and

provide refined information on the statistical characteristics of PD pulses. It may be possible to gain additional insight into the physical bases of the phenomena from the additional information acquired by these new measurements.

This paper discusses three advanced measurement techniques that have been developed at the National Institute of Standards and Technology (NIST). The first is a novel approach for obtaining information about the inherent memory effects associated with PD phenomena and is discussed in Section 2. The second technique employs statistical analysis of PD pulses detected in a cable to locate discharge sites, and is discussed in Section 3. Finally, in Section 4, a measurement technique is described that allows fast photography of PD in liquids and simultaneous broad-band detection of PD current pulses.

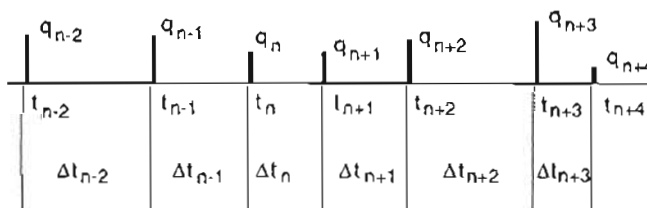


Figure 1.

Diagrammatic representation of the marked random point process corresponding to the Trichel-pulse discharge phenomenon. The Δt_n are pulse time separations and the q_n are pulse amplitudes.

2. MEASUREMENT OF STOCHASTIC PROPERTIES

2.1 BASIC CONSIDERATIONS

PD phenomena fit into a category of stochastic processes for which memory effects play an important role. The existence of memory is an inherent property of PD phenomena because the occurrence of a discharge pulse is associated with the formation of residual ion space charge, surface charges, and metastable excited species that often can affect the initiation and growth of subsequent discharge pulses. As mentioned above, the pulsating characteristic of PD in various types of insulating media can be attributed to effects of space or surface charges. When the accumulation of discharge-generated space or surface charge causes the field to fall below a level sufficient to sustain the discharge, it ceases. Another PD pulse will not occur at this site until the local field is restored such as can result from charge migration or changes in applied voltage.

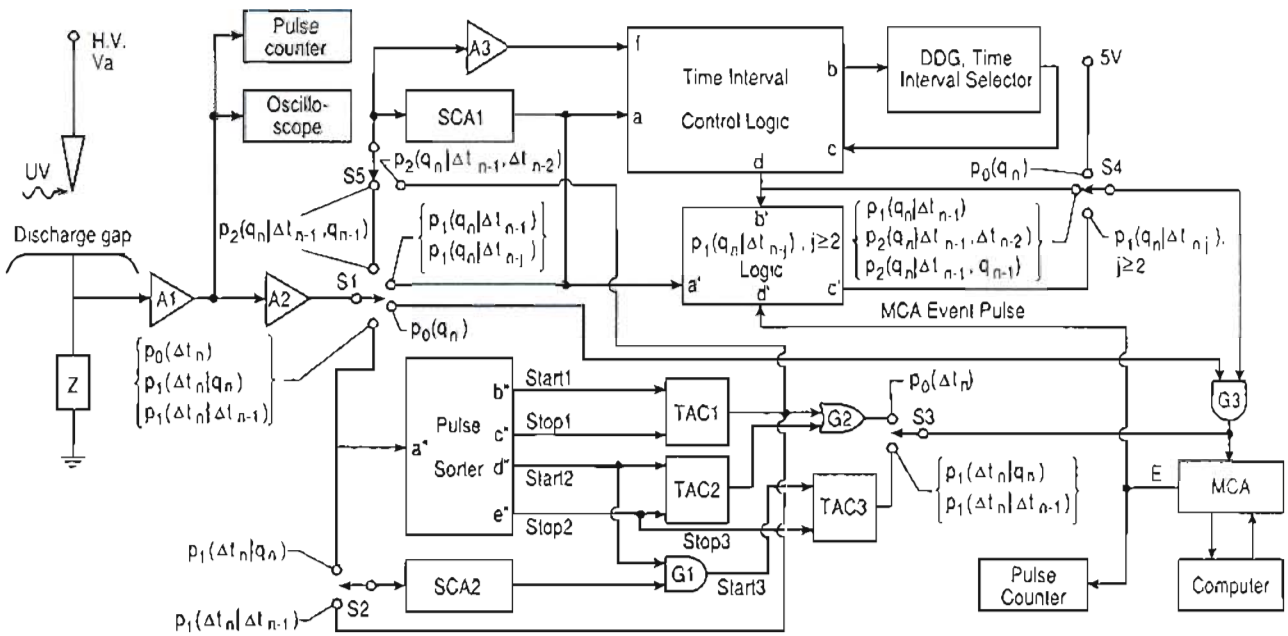


Figure 2.

System for measuring pulse-amplitude and time-separation distributions. In this diagram, the relevant components are identified as follows: MCA - multichannel analyzer; TAC - time-to-amplitude converter; SCA - single channel analyzer; DDG - digital delay generator; A - amplifier; G - gate; and S - switch. Additional details about the individual circuits used can be found in [13].

Because of memory effects, correlations may exist among successive discharge pulses and measurement of these correlations can provide useful information on the nature of PD phenomena. Recognition of this fact motivated the development of a system at NIST to extract information about memory effects. The first version of this system is described in recent publications [13, 14] and has been applied to an investigation of the stochastic behavior of Trichel pulse, negative-corona discharges in electronegative gases [14, 15] and dielectric barrier type discharges in air [16, 39]. A modified version has recently been developed that allows investigation of memory propagation in ac-generated PD phenomena [17]

It is convenient to represent the PD phenomenon as a random point process [18] in which each pulse is identified by a time t_n and is 'marked' with a particular property, in this case the pulse amplitude q_n , as indicated in Figure 1. The stochastic process is thus defined by the set of ordered pairs $\{q_j, t_j\}_k, j = 1, 2, 3, \dots, k$. Because of memory effects, q_n and t_n can depend on the set $\{q_j, t_j\}_{n-1}$, of all previous events, where $j = 1, 2, \dots, n-1$. The process can also be defined by the set $\{q_1, q_j, \Delta t_{j-1}\}_k, j = 2, 3, \dots, k$, where $\Delta t_{j-1} = t_j - t_{j-1}$, which is more appropriate to this discussion since it is the time separations between pulses that are either measured or specified by the measurement process. The pulse amplitude was cho-

sen as the relevant mark because it is a measure of discharge intensity. In defining the point process, one could also consider other marks such as the pulse-shape parameters.

If memory is important in the PD process, the variables $q_n, \Delta t_n, q_{n-1}$ and Δt_{n-1} associated with adjacent events may not be independent. For example, the amplitude q_n may depend on the time separation Δt_{n-1} . Indeed, this is found to be the case for Trichel-pulse discharges [14, 19]. The dependence of Δt_n on q_n or Δt_{n-1} is an indication of the influence of residuals from the previous pulse in either enhancing or retarding the initiation of the subsequent pulse. Likewise, the dependence q_n on Δt_{n-1} or q_{n-1} is an indication of the influence of residuals from the previous pulse on the growth of the subsequent pulse.

Because of these dependencies, the unconditional pulse-amplitude and pulse time-separation distributions, $p_0(q_n)$ and $p_0(\Delta t_n)$ respectively, are not independent. If, for example, an external, radiation source is used to help initiate PD, $p_0(\Delta t_n)$ will change with the intensity of this source since the probability of discharge pulse initiation changes with intensity. The changes in $p_0(\Delta t_n)$ will then be reflected in $p_0(q_n)$ if q_n depends on Δt_{n-1} . Results from measurements of only one distribution, $p_0(q_n)$ or

$p_0(\Delta t_n)$, as are obtained with most conventional PD measurement systems, will be difficult to interpret if memory effects are significant.

The ability to detect correlations among successive discharge pulses is a valuable diagnostic that could be incorporated into existing PD measurement systems either by implementation of filtering techniques similar to those described here, or by off-line analysis of recorded data. The system described below allows 'real-time' measurement of a set of *conditional* pulse-amplitude and pulse-time-separation distributions, namely $p_1(q_n|q_{n-1})$; $p_1(q_n|\Delta t_{n-j})$, $j \geq 1$; $p_1(\Delta t_n|\xi)$, $\xi = q_n$ or Δt_{n-1} ; and $p_2(q_n|\Delta t_{n-1}, \xi)$, $\xi = q_{n-1}$ or Δt_{n-2} . These distributions are defined, for example, such that $p_1(q_n|\Delta t_{n-1})dq_n$ is the probability that the n th pulse has an amplitude in the range q_n to $q_n + dq_n$ if it is separated from the previous pulse by a *fixed* time Δt_{n-1} . The definition of the second-order condition distribution, $p_2(q_n|\Delta t_{n-1}, q_{n-1})dq_n$, is the same but with *both* Δt_{n-1} and q_{n-1} fixed.

By comparison of the measured conditional and unconditional pulse-height and time-separation distributions it is possible to infer immediately whether or not two variables are correlated and therefore dependent. If it is found, for example, that $p_1(q_n|\Delta t_{n-1}) \neq p_0(q_n)$ for at least some allowed values of q_n and for all allowed Δt_{n-1} such that $p_0(\Delta t_{n-1}) \neq 0$, then q_n and Δt_{n-1} are dependent variables. Similarly, if $p_2(q_n|\Delta t_{n-1}, q_{n-1}) \neq p_1(q_n|\Delta t_{n-1})$ for allowed q_{n-1} , then a dependence must exist between q_n and q_{n-1} at a fixed Δt_{n-1} . One can also use the measured conditional distributions to compute correlation coefficients that provide a quantitative measure of the extent to which any two variables in the set $\{q_1, q_n, \Delta t_{n-1}\}$, are correlated.

Measurement of meaningful conditional distributions requires that the PD process be stationary, or at least quasi-stationary. If external factors that affect PD behavior, such as the size of a void, or the electron emission properties of a surface, change during the measurement, the data obtained for conditional distributions could give false indications of possible correlations. The extent to which external factors are important is perhaps best revealed by measurements of the unconditional distributions $p_0(q_n)$ and $p_0(\Delta t_n)$, which can be performed relatively more quickly than the measurements of conditional distributions. The Trichel-pulse corona discharge considered below is an example of a PD phenomenon that is sufficiently stationary to allow measurement of all the conditional distributions for which the system is designed.

2.2 MEASUREMENT SYSTEM

Modifications of the system originally described by

Van Brunt and Kulkarni [13] have been made to:

1. allow direct measurement of the distributions $p_1(q_n|\Delta t_{n-j})$, $j > 2$ and $p_2(q_n|\Delta t_{n-1}, \Delta t_{n-2})$;
2. eliminate intermediate pulse errors associated with measurement of the p_2 distributions;
3. and reduce background associated with accidental sampling of the tails of discharge pulses.

A diagram of the measurement system is shown in Figure 2. This system may be configured to measure any of the indicated distributions by appropriate positioning of the switches (S1-S5). Data from all measurement configurations are accumulated by a 256-channel, computer-controlled multi-channel analyzer (MCA).

The system was first applied to an investigation of the stochastic behavior of negative corona (Trichel pulses) generated using a point-plane electrode gap configuration in electronegative gas mixtures [2]. The test gap is indicated in Figure 2. The corona-discharge current pulses are detected electrically using a preamplifier (A1) connected to an impedance Z that is in series with the discharge gap. The detected pulses are then sent to a variable gain amplifier (A2) before being routed to the appropriate circuit path. For measurement of $p_0(q_n)$, the discharge pulses from A2 are fed directly to the MCA through gate G3, which is kept open by proper positioning of S4.

The distribution $p_0(\Delta t_n)$ is measured by sending the pulses from A2 to a pulse sorter used to trigger two time-to-amplitude converters (TAC1 and TAC2). The time-to-amplitude converters generate output pulses of amplitude proportional to the time between PD pulses. The outputs of TAC1 and TAC2 are fed to the MCA through gate G2 by appropriate positioning of S3. As shown in [13], this arrangement permits the recording of every sequential time interval, provided all time separations exceed the TAC reset time of 50 μ s.

The measurement of $p_1(q_n|\Delta t_{n-1})$ requires use of a logic-controlled digital-delay generator (DDG) to restrict the transfer of pulses from A2 to the MCA to a narrow preselected time interval $\Delta t_{n-1} \pm \delta(\Delta t_{n-1})/2$ for which $\Delta t_{n-1} \gg \delta(\Delta t_{n-1})$. To measure $p_2(q_n|\Delta t_{n-1}, q_{n-1})$, a single-channel analyzer (SCA1) is inserted between A2 and the input to the DDG time-interval control logic circuit by proper positionings of S1 and S5. The SCA1 restricts triggering of the DDG to pulses having amplitudes within the selected range $q_{n-1} \pm \delta(q_{n-1})/2$ for which $q_{n-1} \gg \delta(q_{n-1})$. To insure, in the case of p_2 measurements, that the time-interval control logic properly inhibits the opening of G3 if intermediate pulses occur before the selected time window, it is necessary to modify

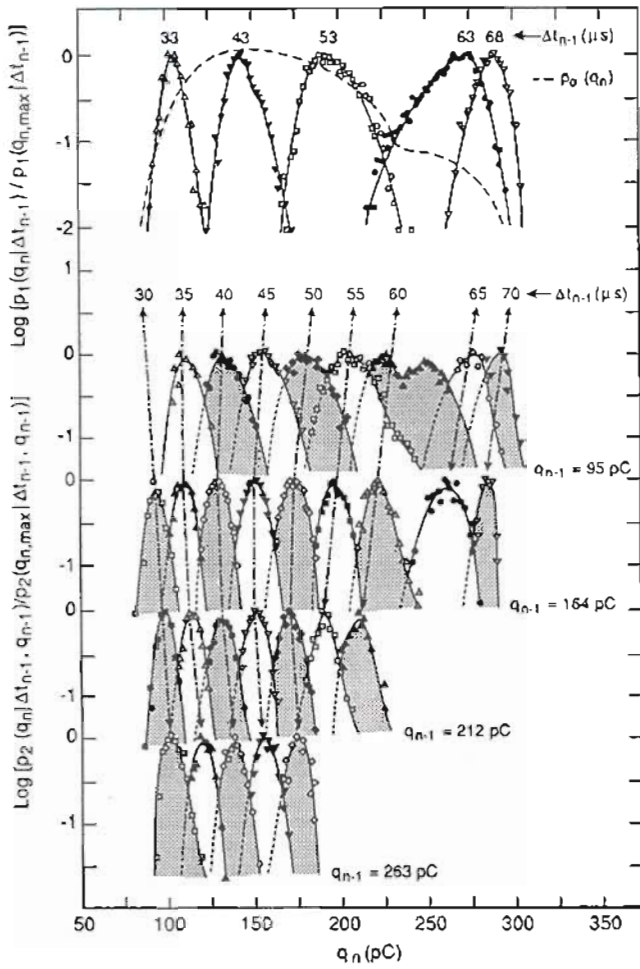


Figure 3.

Measured unconditional and conditional discharge pulse-amplitude distributions $p_0(q_n)$, $p_1(q_n|\Delta t_{n-1})$, and $p_2(q_n|\Delta t_{n-1}, q_{n-1})$ for the indicated fixed values for Δt_{n-1} and q_{n-1} . The distributions have been normalized to the maxima.

the circuit previously described by adding the amplifier A3 with input at f . This amplifier is identical to that defined by transistor T_1 in Figure 2 of [13]. In the present configuration, the input f is connected directly to the delay τ_1 of Figure 2 ([13]), which has, in turn, been disconnected from T_1 .

Unlike the system previously described [13], the present system allows direct measurement of $p_2(q_n|\Delta t_{n-1}, \Delta t_{n-2})$. For measurement of this distribution, the switches S1 and S5 are positioned so that the input to SCA1 is derived from TAC1. The time interval measured by TAC1 is restricted by SCA1 to lie within a narrow range $\Delta t_{n-2} \pm \delta(\Delta t_{n-2})/2$ for triggering the DDG, which, in turn, defines Δt_{n-1} .

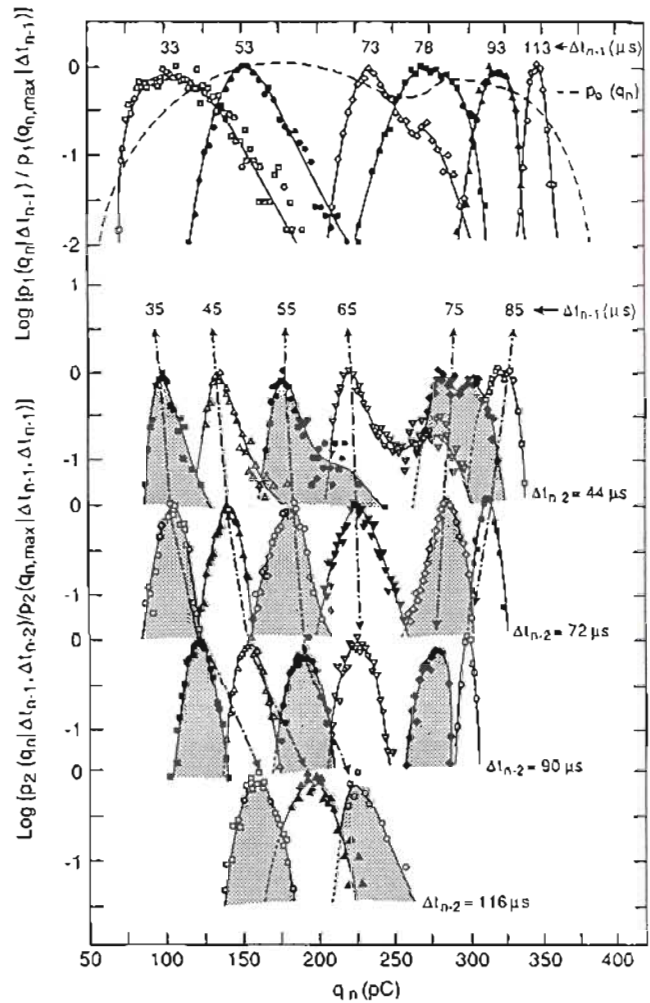


Figure 4.

Measured unconditional and conditional discharge pulse-amplitude distributions $p_0(q_n)$, $p_1(q_n|\Delta t_{n-1})$, and $p_2(q_n|\Delta t_{n-1}, \Delta t_{n-2})$ for the indicated fixed values for Δt_{n-1} and Δt_{n-2} . The distributions have been normalized to the maxima.

By the indicated positionings of switches S1, S2, and S5, it is possible to measure the conditional pulse time-separation distributions $p_1(\Delta t_n|\Delta t_{n-1})$ and $p_1(\Delta t_n|q_n)$. For measurement of $p_1(\Delta t_n|\Delta t_{n-1})$, the output of TAC1 is fed to the input of the single-channel analyzer SCA2 and thus defines Δt_{n-1} and triggers TAC3 for measurement of the next time interval Δt_n . In the case of the $p_1(\Delta t_n|q_n)$ measurement, SCA2 is connected directly to amplifier A2 thereby used to define q_n .

The present system also differs from that previously described in that the $p_1(q_n|\Delta t_{n-j})$ logic circuit now contains a pulse counter that can be set for any $j \geq 2$. By adjustment of the delays inherent to the time-interval

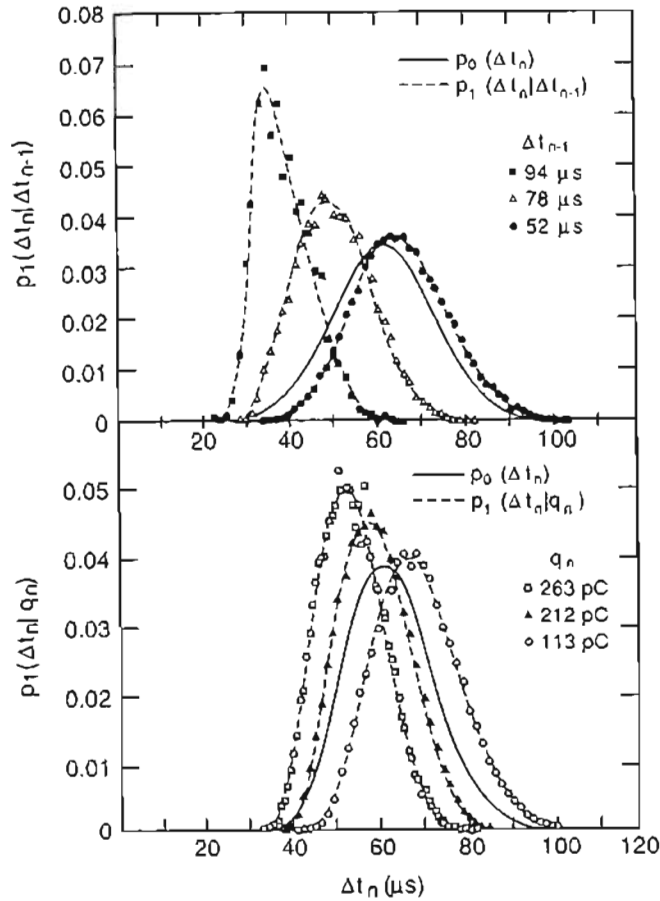


Figure 5.

Measured unconditional and conditional discharge pulse-time-separation distributions $p_0(\Delta t_n)$, $p_1(\Delta t_n|q_n)$, and $p_1(\Delta t_n|\Delta t_{n-1})$ for the indicated fixed values for q_n and Δt_{n-1} . The distributions have been normalized to the areas under the curves.

control logic and with minor adjustments in the shape of the gate pulse from this circuit, it has been possible to largely eliminate the background problem illustrated by Figure 5 of [13].

In the present measurement system, the pulse detection circuit conditions are similar to those described in [13] so that the measured discharge-pulse amplitude is proportional to the net charge transported in the discharge given by

$$Q'_n = \int_{-\infty}^{\infty} i_n(t) dt \quad (1)$$

where $i_n(t)$ is the instantaneous discharge current at time t for the n th pulse. Given the impulse response $h(t-t')$ of the detection circuit (defined here mainly by the filter

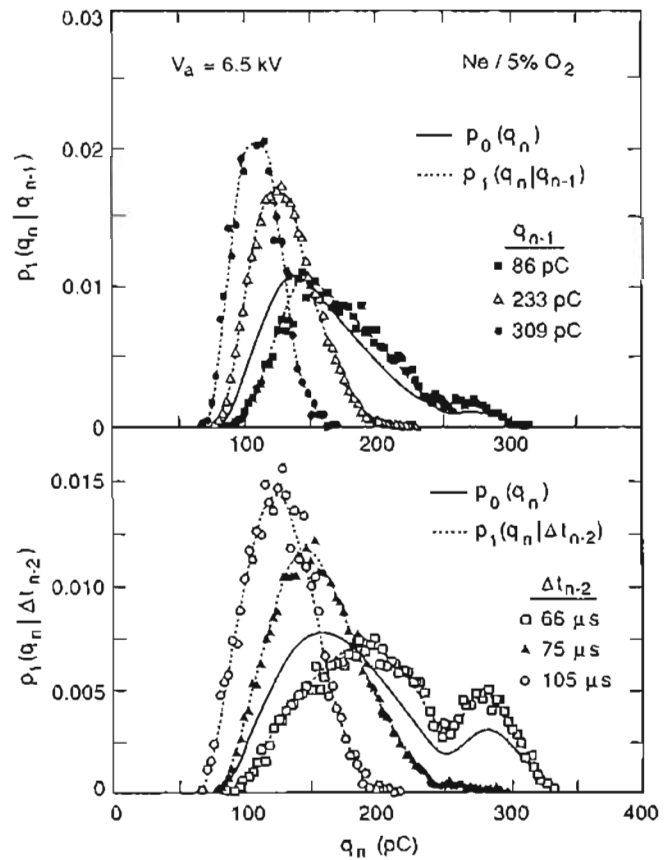


Figure 6.

Measured unconditional and conditional discharge pulse-amplitude distributions $p_0(q_n)$, $p_1(q_n|\Delta t_{n-2})$, and $p_1(q_n|q_{n-1})$ for the indicated fixed values for Δt_{n-2} and q_{n-1} . The distributions have been normalized to the areas under the curves.

characteristics of Z and A1), the observed pulse signal is given by

$$q'_n(t) = \int_{-\infty}^t i_n(t') h(t-t') dt' \quad (2)$$

The impulse response in the present measurement system has a width, w_i of $\sim 1.5 \mu s$ whereas the intrinsic width w_p of a typical Trichel pulse is known [9] to be on the order 10 to 50 ns. Therefore the condition $w_i \gg w_p$ allows the approximation

$$i_n(t) \simeq Q'_n \delta(t-t_n) \quad (3)$$

where $\delta(t-t_n)$ is the Dirac delta function. Using this in Equation (2) gives

$$q'_n(t) = Q'_n h(t-t_n) \quad (4)$$

This means that the shapes of the observed Trichel pulses in the present experiment are governed primarily by the

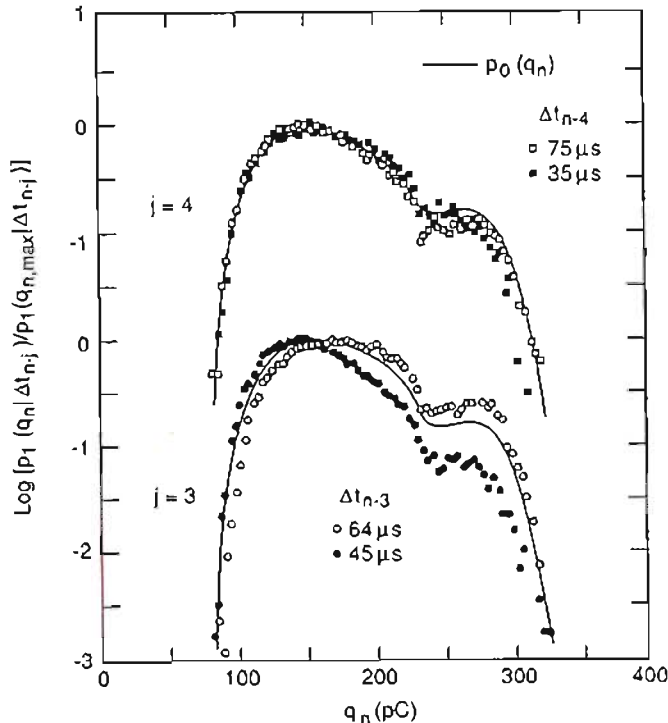


Figure 7.

Measured unconditional and conditional discharge pulse-amplitude distributions $p_0(q_n)$, $p_1(q_n|\Delta t_{n-3})$, and $p_1(q_n|\Delta t_{n-4})$ for the indicated fixed values for Δt_{n-3} and Δt_{n-4} . The distributions have been normalized to the maxima.

shape of $h(t-t_n)$ and thus the maximum of $q'_n(t)$, denoted here by q_n , is directly proportional to Q'_n . Therefore, q_n can be expressed in units of charge, and in the present case, it is convenient to use pC. The method for calibrating the pulse-height measurements in terms of charge is the same as described previously [8].

2.3 EXAMPLES OF RESULTS FROM INVESTIGATION OF TRICHEL PULSES

The Trichel-pulse discharge [20] was selected for initial test of the measurement concept because its properties are reasonably well understood [22-25] and it can be easily generated and controlled in a simple point-plane gap. With some care, the Trichel-pulse discharge can be maintained in a stable condition for relatively long periods of time. The phenomenon is shown [14] to be a clear example of a non-Markovian, marked random point process in which memory effects play an important role.

Strong correlations are found to exist among the amplitudes and time separations of successive discharge pulses, which can be interpreted in terms of the influences of ion space charge and metastable species from previous pulses on the initiation and growth of subsequent pulses.

As an example of the richness of information that can be extracted with the present measurement system, results obtained for self-sustained Trichel pulses in a neon-oxygen gas mixture are shown in Figures 3 to 7. Data for the different sets of distributions were obtained at different times so that the cathode surface conditions that apply, for example, to the results in Figure 3 differ slightly from those that apply to Figure 4. This accounts for the difference in $p_0(q_n)$ shown in these two Figures. A detailed interpretation of the results presented here would go beyond the scope of this report. However, salient features of the data and certain important conclusions that can be derived therefrom should be noted. A more complete discussion of the physical bases for the stochastic behavior of the Trichel-pulse phenomenon has been given by Van Brunt and Kulkarni [14].

The fact that the second-order conditional distributions, p_2 , differ from the corresponding first-order distributions, p_1 , which in turn differ from the corresponding unconditional distributions, p_0 , indicates unequivocally that the set of variables $\{\Delta t_n, q_n, \Delta t_{n-1}, q_{n-1}, \Delta t_{n-2}, \dots\}$ associated with adjacent pulses are not independent. For example, it is seen from Figures 3 and 4 that q_n has a strong positive dependence on Δt_{n-1} . This dependence can be related to the influence of negative-ion space charge from previous pulses in suppressing the magnitude of the electric field at the cathode when the next pulse develops. It is also seen from Figure 3 that the amplitude q_n of a pulse can be either positively or negatively dependent on the amplitude of the previous pulse. The sign of this dependence can be explained in terms of the competing effects of negative-ion space charge and metastable species in respectively retarding or enhancing the growth of the next pulse. The negative dependence of Δt_n on q_n (and Δt_{n-1}) implied by the conditional time-separation distributions shown in Figure 5 can be understood in terms of the influence of metastable species from the previous pulse in enhancing the probability for initiating the next pulse by ejecting electrons from the cathode surface during field-assisted quenching.

Because of the correlations among the amplitudes and time separations of successive pulses, the distributions shown in Figures 3 to 5 are all related. It can be shown, for example, from the law of probabilities that $p_0(q_n)$, $p_0(\Delta t_n)$, and $p_1(q_n|\Delta t_{n-1})$ are related by the integral

expression

$$p_0(q_n) = \int_0^\infty p_0(\Delta t_{n-1}) p_1(q_n | \Delta t_{n-1}) d(\Delta t_{n-1}) \quad (5)$$

and that the distributions $p_0(q_n)$, $p_0(\Delta t_n)$, $p_1(q_n | \Delta t_{n-1})$, $p_1(\Delta t_n | q_n)$, and $p_2(q_n | q_{n-1}, \Delta t_{n-1})$ are related by

$$p_0(\Delta t_{n-1}) p_1(q_n | \Delta t_{n-1}) = \int_0^\infty p_0(q_{n-1}) p_1(\Delta t_{n-1} | q_{n-1}) p_2(q_n | q_{n-1}, \Delta t_{n-1}) dq_{n-1} \quad (6)$$

Equation (5) indicates that if q_n is dependent on Δt_{n-1} , then any externally-induced change in the time-interval distribution, $p_0(\Delta t_n)$, will necessarily change the amplitude distribution, $p_0(q_n)$.

Since, as seen from the data in Figures 4, 6, and 7, the profiles for $p_2(q_n | \Delta t_{n-1}, \Delta t_{n-2})$ and for $p_1(q_n | \Delta t_{n-j})$, $j = 2, 3, 4$ do not match the profile for $p_0(q_n)$, it can be stated that q_n depends on Δt_{n-j} , $j > 1$, and therefore, the process is one for which memory extends back in time beyond the most recent event, i.e., the process is non-Markovian. This observation is consistent with results reported in the recent work of Steiner [19]. It can, in fact, be shown [14] that, because of the relatively strong dependence of q_n on both Δt_{n-1} and q_{n-1} , it is possible for memory to propagate indefinitely back in time. Recent measurements [16, 39] in our laboratory have shown that, for Trichel pulse discharges, additional memory associated with the deposition of surface charge on an insulating surface occurs when a thin circular dielectric is placed on the planar anode surface in the point-plane discharge gap. The existence of memory effects associated with charging of insulated surfaces has also been verified for ac-generated PD [17].

2.4 LIMITATIONS AND EXTENSIONS OF THE TECHNIQUE

It should be realized that the system, as shown in Figure 2, has certain limitations. First, it is designed to operate with dc voltages. Second, as discussed in [13], it cannot give reliable measurements of certain conditional distributions if the time separations between events become shorter than either the TAC reset time or the MCA analog-to-digital conversion time. Third, it cannot be applied to nonstationary phenomena that drift on a time scale comparable to the time required to acquire

statistically significant data. Fourth, it can only measure one distribution at any given time. Fifth, independent of the problems associated with timing in either the TAC or MCA, the ability to resolve pulses is limited by the width of the impulse response and therefore the band-width of the detector. Because of this limitation, it could not, for example, be applied to investigate bursts of closely spaced PD pulses, which, as shown below, occur in liquids and are known to occur in the positive corona of some electronegative gases like SF₆ [8].

The restriction to dc voltages can be overcome by incorporating a phase marker such as a zero-crossing sensor to identify the phase associated with any given pulse time separation. The system has, in fact, been recently modified to allow measurement of conditional distributions restricted to specific phase intervals [17]. For example, it now allows measurement of the phase-conditioned distributions, $p_1(q_i(\phi_i) | \Delta\phi_j)$, where q_i is the amplitude of any PD pulse that occurs with phase ϕ_i contained in the specified interval $\Delta\phi_j$. This type of distribution has been considered recently by others [11, 12]. However, in addition to this distribution, our system is capable of measuring many others in which phase is specified and from which effects of memory propagation can be assessed. These include the distributions $p_1(q_1(\Delta\phi_2^\mp) | Q(\Delta\phi_1^\pm))$ and $p_1(\phi_1^\pm | Q(\Delta\phi_1^\pm))$, where q_1 and ϕ_1 are respectively the amplitude and phase of the first pulse to occur in either the positive or negative half-cycle specified respectively by the phase intervals $\Delta\phi_2^\mp$ or $\Delta\phi_2^\mp$ and

$$Q(\Delta\phi_1^\pm) = \sum_j q_j(\phi_j^\pm) \quad \phi_j^\pm \in \Delta\phi_1^\pm \quad (7)$$

is the total charge associated with all PD pulses occurring within phase interval $\Delta\phi_1^\pm$ of the preceding half-cycle. Preliminary data obtained on these distributions for dielectric barrier discharges at frequencies from 60 to 200 Hz show that the charge deposited on a dielectric surface by PD during one half-cycle significantly affect the onset and development of PD during the subsequent half-cycle.

Limitations on minimum time separations can be overcome in principle by using prerecorded data that can be obtained with fast-transient digitizers. However, if prerecorded data are to be used, it may be preferable to determine the conditional distributions with computer software rather than with the hardware presented here. It should be emphasized that an important advantage of the hardware approach described here is that the conditional distributions can be measured and viewed in *real time*. This is an advantage not only because it gives an immediate visualization of the results while data are recorded, but because it overcomes the problem of having to

store enormous quantities of data required to determine conditional distributions by the software approach. For example, some of the second-order conditional distributions shown in Figures 3 and 4 required ≈ 10 min of data acquisition time in order to obtain acceptable statistics. This means that data on all but a very small fraction of the discharge events that occurred in this ten minute period were discarded by the filtering procedure. Using the software approach, all the pulses that occurred during that time would have to be stored, which means that for the data shown more than 10^9 pairs of numbers would have to be acquired just to determine one distribution.

If the PD phenomenon is, or can become, nonstationary, then an independent method may be needed to determine the extent to which it is nonstationary. A periodic check of the unconditional pulse amplitude and/or time separation distribution will, in some cases, provide an indication of deviations from stationary behavior.

In the case of multiple PD discharge sites, an ambiguity can occur in the interpretation of data from measurement of conditional distributions, particularly if the discharges from the different sites occur with nearly equal intensity. The measurement scheme discussed here works best if there is only one site at which PD discharges are being generated with an intensity that is significantly above the background PD level. The existence of pronounced correlations among successive PD pulses would, in fact, indicate that the discharges are occurring at one, or a limited number of sites. The determination of this fact might be important in some diagnostic applications.

Finally, it should be pointed out that the present system could be modified to allow a more efficient use of the available data. One could, for example, use multiple MCA's in parallel to measure more than one distribution simultaneously.

3. LOCATION OF PARTIAL DISCHARGES IN CABLES

LOW-VOLTAGE cables, in contrast with those designed for HV service, are not free from PD under moderate overvoltage conditions. Therefore, the occurrence of a PD at an incipient defect must be differentiated from a large background of PD that occur along the length of cable. The methods [26] described in this Section allow discharge sites associated with insulation breaches to be located with high efficiency. To demonstrate the utility of these methods, three representative types of cables having artificially introduced defects were subjected to test; in each case the defects were successfully located.

The approach is similar to that previously considered by others [4, 27, 28].

3.1 BASIC PRINCIPLES

If voltages exceeding the PD threshold are applied to a cable, PD can occur along the entire length of a cable. Therefore, methods must be developed that are sensitive to the location of the discharge and the level of activity at each site.

It is reasonable to assume that, in the absence of defects, PD sites are uniformly distributed over the length of cable, and that PD at different sites are not correlated in time. The discharges thus define a marked, random point process that asymptotically resembles Poisson shot noise [18, 19], with pulses emanating from all positions along the cable.

If it is further assumed that the pulse amplitudes at each site are gamma-distributed [26] with the parameters of the probability density being independently and identically distributed, then the probability density for a pulse of amplitude q will have the form

$$p_0(q) = \int_{z,w} p_2(q|z, w) p_0(z) p_0(w) dz dw \quad (8)$$

$p_2(q|z, w)$ is a conditional probability density of the charge at a single site, $p_0(z)$ is the probability density of discharge sites and $p_0(w)$ is the probability density of the parameter w which controls the most probable discharge amplitude at a site. Superposition of these infinitesimal processes yields a well behaved, unimodal probability density $p_0(q)$.

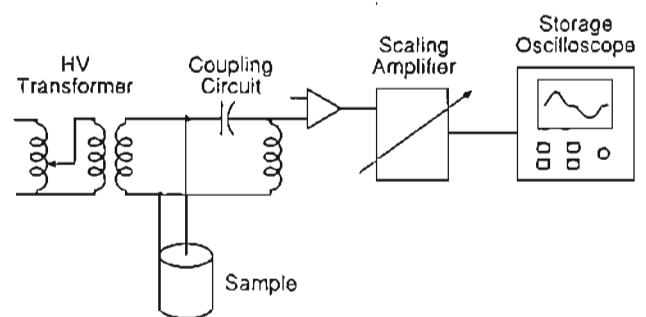


Figure 8.

Block diagram of partial discharge detection and recording apparatus.

Significant deviation from the behavior defined by Equation (8) may be used to identify defects sites. The effects of defects may be included by adding terms in which

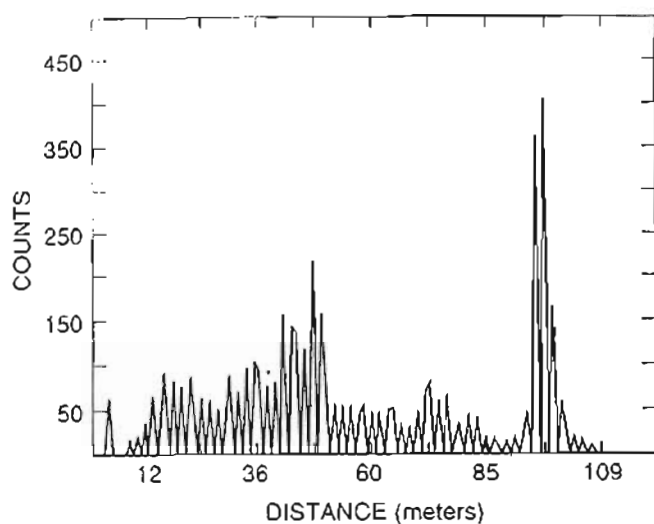


Figure 9.

Histogram of delay times between the two major pulses in each event of a 5000 element record containing true pairs and random pairs.

$p_0(w)$ is replaced by $p_1(w|z)$, where w depends on z and is highly localized to particular points z_i . For this case, Equation (8) is rewritten as

$$p_0(q) = Pr(z \neq z_i) \int_{z,w} p_2(q|z, w) p_0(z) p_0(w) dz dw + [1 - Pr(z \neq z_i)] \sum_{i=1}^N \int_w p_2(q|z_i, w) p_1(w|z_i) Pr(z = z_i) dw \quad (9)$$

where $1 - Pr(z \neq z_i)$ is the probability that a PD is from one of the N defect sites namely at the i th site.

The measurement concept has merit if the PD behavior at the defects differs substantially from that due to the normal background of PD in the cable. If a flaw is detectable, a histogram of the discharge locations will exhibit a sharp peak. Furthermore, the sensitivity to PD at defects can be enhanced by pulse-height discrimination, so that only anomalously large PD are detected. In practice, there will be naturally occurring, apparent PD sites that are not associated with flaws but cause variations in the expected background count rates. In fact two such locations can be identified with the ends of the cable where reflections of the PD signals can occur.

3.2 EXPERIMENTAL APPARATUS

The experimental apparatus, shown in block diagram form in Figure 8, consists of a HV system, a coupling

circuit and instrumentation that allow acquisition and analysis of broadband PD waveforms. HV is provided by a 60 Hz transformer with appropriate noise filtering.

The cable under test is connected to the measurement system through a coaxially mounted 1 nF capacitor, the first element in a high-pass filter having a lower cutoff frequency of 30 kHz and a 1000 Ω input impedance. For the purposes of this study, threshold is defined as that voltage for which one PD pulse is detected per second. Initial tests yielded PD amplitudes > 10 pC at the threshold voltage, and thus an input attenuator and protective circuitry were added. The protective circuit limits the input sensitivity to 1 pC and the bandwidth of the system to ≈ 10 MHz. A variable attenuator is included between the input preamplifier and the gain block to provide amplitude scaling and prevent saturation of the amplifier.

PD pulses are recorded on a digital oscilloscope and transferred to a computer for mass storage and processing. The oscilloscope used for this study has an 8-bit digitizer and a sampling rate of 10^8 samples/s. Typically, 5000 waveforms are collected during each test. Data collection can be completed in only a few seconds, however, voltage is typically applied for 8 minutes since the HV system is not computer controlled and time is needed to archive the data. A computer with only moderate computational power is used and all signal processing is performed off line.

3.3 MEASUREMENTS

Two fundamental estimates are made from each recorded waveform: the charge, and the location of the PD. The method used to estimate the charge is described by Steiner and Weeks [29] and has been shown to be more accurate than the usual peak value measurement. The technique derives a pulse energy from the measured waveform and estimates the total charge from the energy. The PD waveform is assumed to be similar to a calibration pulse, generated by applying a fast-rise step voltage of known amplitude through a known capacitance to the cable under test. Inclusion of the effects of cable attenuation in the charge estimate were not deemed necessary for this study.

When a PD occurs, two pulses, which travel along the cable in opposite directions, are generated. One pulse proceeds toward the detector and arrives at time t_1 . The second pulse is reflected from the open circuit, back toward the detector, and arrives at time t_2 . Thus the location of the discharge relative to the open cable end, l , is

given by

$$l = \frac{v(t_2 - t_1)}{2} \quad (10)$$

where v is the velocity of propagation.

A matched filter whose shape approximates a PD pulse is applied to the recorded waveform. In effect, an assumed pulse is cross-correlated with the recorded waveform, and the time delay between the two largest pulses is converted to a location. This method has two limitations: The two largest pulses within a record may be from distinct discharge sites, thus a false location is determined. In most cases, however, false signals tend to be randomly distributed along the cable length. The second limitation is associated with the existence of a blind spot in the cable. When the arrival times of the direct and reflected pulses are nearly the same it is difficult to differentiate between a single pulse and two closely spaced pulses. Without extensive signal processing, these sites all appear to be near the end of the cable, in effect creating a blind spot.

3.4 TEST RESULTS

The measurement technique was tested using representative 600 V class cables. These cables may be grouped into three categories: shielded cables, unshielded multi-conductor cables, and unshielded single conductor cables. The following samples were used in a series of experiments:

1. An unaged, unshielded, two-conductor, #14 AWG, 600 V class, neoprene jacketed cable of the same type used for control cabling in nuclear power plants.
2. An unaged, 50 Ω , coaxial cable of the same type used for instrumentation cabling in nuclear power plants.
3. An aged, unshielded, 15 conductor, #18 AWG cable of the same type used for instrumentation cabling in nuclear power plants.

No experiments were conducted on unshielded single-conductor cables since this technique requires that the cable have some transmission line properties; a single conductor, in the absence of a ground plane, does not.

Tests were performed on a 100 m length of unaged, two-conductor cable with defects introduced at three locations. A small portion of the jacket was removed and the insulation was carefully pierced through to the conductor using a #60 twist drill at two of the locations, and a razor knife was used to slit the insulation at the third. The PD threshold for the cable was 4500 V and measurements were made at voltages levels 10, 20, and

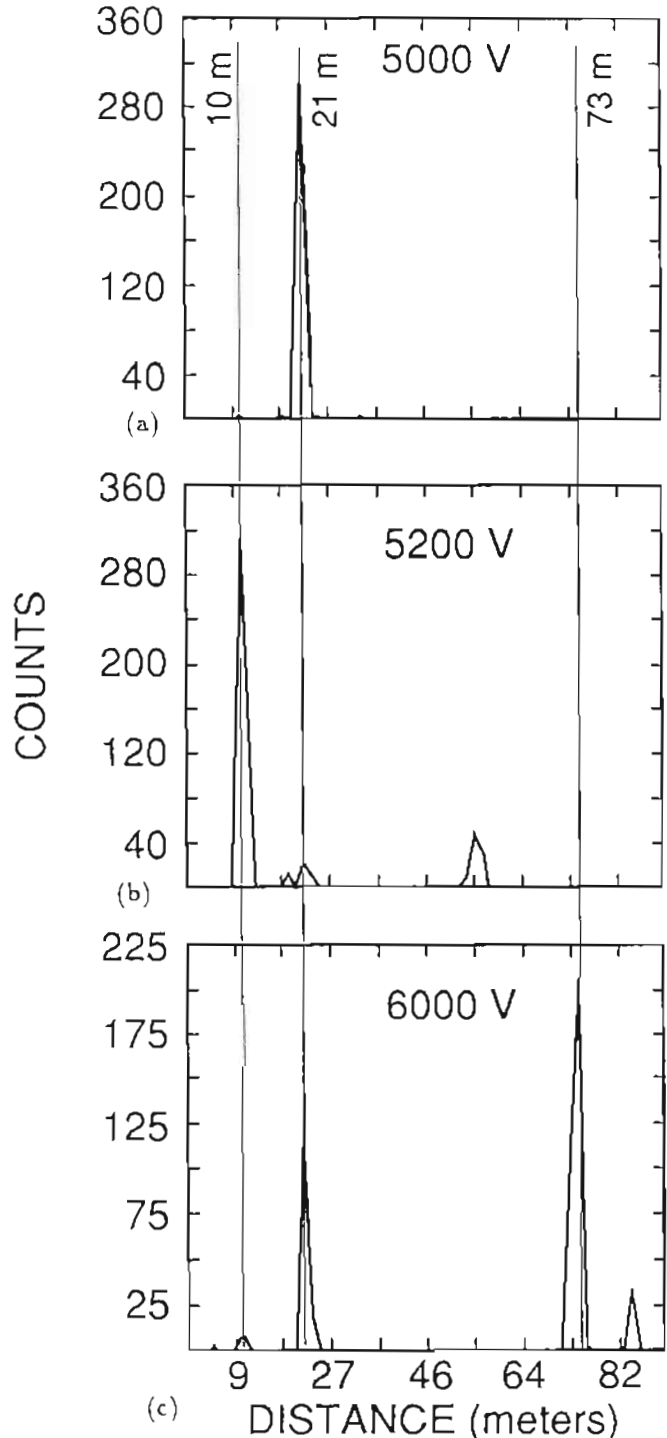


Figure 10.

Histogram of time delays for (a) 5000 V, (b) 5200 V and (c) 6000 V.

40% above threshold. Representative data from these tests are shown in Figure 9. The data plotted in Figure 9 are obtained for a relatively low trigger level, consequent-

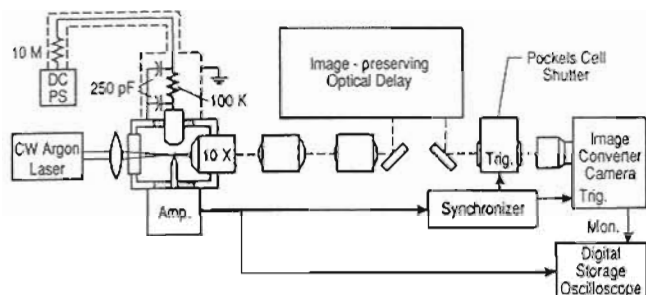


Figure 11

Schematic diagram of the experimental apparatus used for simultaneous fast photography and current measurements.

ly background PD are dominant. Note that the PD are reasonably evenly distributed along the length of the cable, which lends support to the model presented above. Sensitivity to PD at a damage site may be enhanced by increasing the trigger level, as is the case for the data plotted in Figure 10. The damage sites were found using the delay values that correspond to the peaks in the charge histograms shown in Figure 10; each of the damage sites was correctly identified.

Similar measurements were made on a 20 m length of coaxial cable with damage inflicted by slightly abrading the shield. The PD threshold was 5200 V. The PD activity at the damage site was much greater than that of the background and the defect was immediately identified. Similar results were obtained for a 12 m length of aged multiconductor cable with a defect created in the cable by cutting the insulation on one of the 15 conductors. The PD threshold voltage for this cable was 2300 V. As in the previous case, the PD activity at the damage site was much greater than the background and the location of the defect was readily identified.

4. MEASUREMENT OF PARTIAL DISCHARGE IN LIQUIDS

METHODS are described here that allow simultaneous measurement of PD current and fast photography of the discharge. Such data allow detailed description of the temporal and spatial development of the PD and provide a basis for evaluation of models for the initiation of the discharge. To demonstrate these methods, experimental results obtained during a study of hexanes [35] are briefly discussed. A non-uniform field geometry was employed for these measurements and cavitation associated with PD at a negative point was photographed using shadowgraphic methods.

Photographic and optical studies [30-33] have established a clear correspondence between current emitted from a negative point electrode, which is typically observed as a burst of fast discharge pulses, and cavitation at the electrode. Further study of these effects may prove useful in identifying the conditions that lead to the initiation of PD and electrical breakdown in dielectric liquids. The PD phenomena examined here bear strong resemblance to the initial growth of negative streamers. Electric breakdown of dielectrics liquid is preceded by characteristic prebreakdown phenomena: the growth of a streamer in the liquid. An analysis of streamer growth presented by Watson and Chadband [34] shows the initial growth of negative streamers to be consistent with the propagation of a cavity within the liquid.

4.1 EXPERIMENTAL APPARATUS

The experimental apparatus is shown schematically in Figure 11. The test gap consists of a steel needle and stainless steel rod separated by 3.2 mm. The rod electrode is 6.4 mm in diameter and has a hemisphere of the same diameter at its tip. The radius of the needle tip is $\approx 1 \mu\text{m}$, and the apex angle is approximately 30° . The electrodes are enclosed within a brass cell and are immersed in the test liquid.

High-resolution images of the PD are obtained by mounting a microscope objective within the cell. This configuration provides optical resolution of $< 2 \mu\text{m}$ at $200\times$ magnification. A continuous wave argon laser is used to illuminate the region near the tip of the needle: light is scattered from the laser beam as the cavity grows and an image of the PD may be recorded photographically. In the present study, a fast-framing camera is used to photograph the PD, thus a record of the spatial and temporal development of the PD is obtained. The image-preserving optical delay [32,36], noted in Figure 11, offsets the camera trigger delay and allows the framing sequence to begin much closer to, and, for some frame intervals, before the current waveform. Use of the optical delay has an additional benefit: Since, near the threshold for PD activity, discharges occur infrequently, ordinary photographic methods are ineffective in capturing the discharge. Use of the optical delay, however, allows the camera to be triggered by the discharge current and thus provides a highly efficient method for photographing PD.

A broadband transimpedance amplifier [37] is connected directly to the needle electrode and the current waveform is recorded on a digital oscilloscope. The amplifier has a bandwidth of 35 MHz, an equivalent noise

of 30 nA rms, and an estimated charge sensitivity of < 0.7 fC. The amplifier gain is 10^5 V/A. The rod electrode is connected to a HV dc power supply, and, for the results presented here, 15.5 kV is applied. A 10 MΩ series resistor is included to limit the current in the event of breakdown. The filter circuit shown in the Figure is provided to reduce pickup of power supply noise.

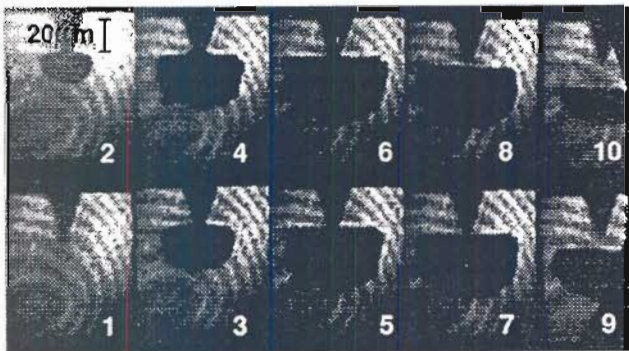
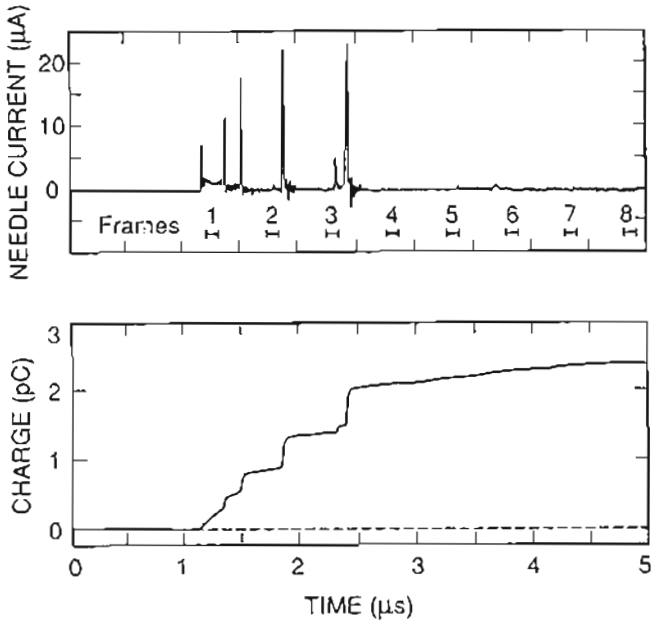


Figure 12.

PD record. The current waveform and the integrated charge are shown together with frame photographs of the point cathode. These data are obtained for an applied potential of 15.5 kV in hexanes. The frame interval and exposure times are 512 and 102 ns respectively. The frame sequence is indicated in the photograph.

4.2 PARTIAL DISCHARGE RECORDS

An example of a PD is shown in Figure 12. The current waveform and the integrated current are plotted in the

upper panels and the associated multi-frame photograph is shown below. The frame interval and exposure times are 512 and 102 ns respectively, and the frame sequence is indicated in the Figure. The frame exposures, determined from the camera monitor pulse and an accurate measurement of the frame interval, are shown together with the current waveform. The interference rings appearing in the photographs are an artifact of the coherence of the laser light and should be disregarded.

The dynamical behavior of these structures is particularly intriguing. During its lifetime, the cavity first grows in size, then detaches from the needle, and finally breaks apart and collapses, moving away from the tip as it collapses. Although a great deal of variability is observed in the detailed growth, common patterns are observed. The structure appears to be approximately spherical at inception and may grow by stable expansion, as is shown in Figure 12, or by the growth in amplitude of instabilities in the cavity wall. Upon close examination, evidence for the onset of instabilities may be seen in Figure 12.

The PD current waveform is relevant to describing the conditions at the initiation of the discharge. Consistent with earlier work [30, 31, 37, 38], fast PD pulses are seen to occur during the growth of the cavity. It was further noted during this study that a continuous current occurs near the initiation of the waveform in a large fraction of the recorded waveforms: the data shown in Figure 12 is representative of this behavior. Motion of space charge trapped in the liquid due to the expansion of the cavity would give rise to a continuous current. Additionally, whereas the amplitude of the latter pulses tends to grow monotonically and appears to correlate with the size of the cavity at a given instant, the first two pulses were frequently of comparable amplitude. Indeed, PD were observed that consisted of only a double-pulse structure. Single current pulses were also detected; however, no evidence of cavity growth could be seen in the associated photographs.

The frame photographs may be used, for example, to estimate the average rate of expansion of the cavity and, therefore, the effective pressure within the cavity. Such an estimate yields pressures on the order of 0.4 MPa [35]. The required pressure may be provided by electrical discharges within the cavity and the subsequent heating of the vapor within the cavity and the surrounding liquid, and by electrostatic forces. The form of the cavity, however, suggests that the forces acting on the liquid are highly directional, and thus that the gas dynamic pressure is of limited importance. This observation may lend support to the results of Watson and Chadband [34] who argue that electrostatic forces play a predominant role in driving the expansion of the cavity.

5. SUMMARY

THIS paper has described three different PD measurement techniques developed at NIST. The first is a novel approach for obtaining information about the inherent memory effects associated with the stochastic behavior of PD phenomena. It is shown that determinations of the correlations among successive discharge pulses can provide valuable supplementary information about the physical mechanisms of PD, and such information will be quite useful for diagnostic purposes in practical applications. The second technique concerns the detection of PD along a cable and offers a method for assessing the likelihood of a fault due to an incipient defect, such as a breach of the insulation that would remain undetected under normal operating conditions. The method described here may be readily adapted to process manufacture, to ensure the quality and reliability of critical components, and to the assessment of complex electrical systems in-situ.

With the third measurement technique described here, highly resolved photographs of the initiation of PD in liquids can be obtained. Such photographs show, for example, that the discharge cavity growth at a negative point in hexanes is nonisotropic, which suggests that electrostatic forces are of primary importance in driving its expansion. The onset of instabilities in the cavity wall is suggested. The optical observations are correlated with simultaneous fast electrical measurements of the PD current pulses. The current pulses are seen to occur intermittently during growth of the cavity and appear to be correlated in amplitude with the size of the cavity.

ACKNOWLEDGEMENT

THIS work is supported in part by the Office of Energy Storage and Distribution, Electric Energy Systems Program, US Department of Energy and by the Nuclear Regulatory Commission. The research described here is a result of the efforts of many researchers, in particular, we wish to acknowledge T. V. Blalock, E. W. Cernyar, C. Fenimore, E. F. Kelley, F. Martzloff, M. O. Pace, A. L. Wintenberg, and H. Yamashita, who have each greatly contributed to these efforts.

REFERENCES

- [1] R. Bartnikas, "Detection of Partial Discharges (Corona) in Electrical Apparatus", IEEE Trans. Electr. Insul., Vol. 25, pp. 111-124, 1990.
- [2] L. B. Loeb, *Electrical Coronas - Their Basic Physical Mechanisms*, University of California Press, pp. 26-40, 1965.
- [3] R. S. Sigmond, "Corona Discharges", in *Electrical Breakdown of Gases*, Ed. by J. M. Meek and J. D. Craggs, John Wiley and Sons, pp. 319-384, 1978.
- [4] R. Bartnikas, "A Commentary on Partial Discharge Measurement and Detection", IEEE Trans. Electr. Insul., Vol. 22, pp. 629-653, 1987.
- [5] F. H. Kreuger, *Discharge Detection in HV Equipment*, Elsevier NY, 1965.
- [6] R. Bartnikas, "Use of Multichannel Analyzers for Corona Pulse Height Distribution Measurements in Cables and Other Electrical Apparatus", IEEE Trans. on Instrum. and Measurement, Vol. 22, pp. 403-407, 1973.
- [7] R. Bartnikas, "Corona Pulse Counting and Pulse Height Analysis Techniques", in *Engineering Dielectrics*, Vol. 1, eds. R. Bartnikas and E. J. McMahon, STP 669; ASTM Press, Philadelphia, pp. 285-326, 1979.
- [8] R. J. Van Brunt and D. Leep, "Characterization of Point-Plane Corona Pulses in SF₆", J. Appl. Phys., Vol. 52, pp. 6588-6600, 1981.
- [9] S. V. Kulkarni and R. S. Nema, "Broad Band Pulse Detection Studies of Corona and Breakdown in Air, N₂, O₂, CO₂, SF₆, and SF₆-N₂ Mixtures", in *Gaseous Dielectrics V*, Ed. by L. G. Christophorou and D. W. Bouldin, Pergamon Press NY, pp. 637-642, 1987.
- [10] R. J. Van Brunt and M. Misakian, "Mechanisms for Inception of dc and 60 Hz ac Corona in SF₆", IEEE Trans. Electr. Insul., Vol. 17, pp. 106-120, 1982.
- [11] H. Hikita, Y. Yamada, A. Nakamura, T. Mizutani, A. Oohasi, and M. Ieda, "Measurement of Partial Discharges by Computer and Analysis of Partial Discharge Distribution by the Monte Carlo Method", IEEE Trans. Electr. Insul., Vol. 25, pp. 453-468, 1990.
- [12] J. Fuhr, M. Haessig, B. Fruth, and T. Kaiser, "PD-Fingerprints of Some HV Apparatus", Conference Record of the 1990 IEEE International Symposium on Electrical Insulation, Toronto Canada, pp. 129-132, 1990.
- [13] R. J. Van Brunt and S. V. Kulkarni, "Method for Measuring the Stochastic Properties of Corona and Partial-Discharge Pulses", Rev. Sci. Instrum., Vol. 60, pp. 3012-3023, 1989.

- [14] R. J. Van Brunt and S. V. Kulkarni, "Stochastic Properties of Trichel-Pulse Corona: A Non-Markovian Random Point Process", *Phys. Rev. A*, Vol. 42, pp. 4908-4932, 1990.
- [15] R. J. Van Brunt and S. V. Kulkarni, "New Method for Measuring the Stochastic Properties of Corona and Partial Discharge Pulses", *Conference Record of the 1988 IEEE International Symposium on Electrical Insulation*, New York NY, pp. 233-237, 1988; S. V. Kulkarni and R. J. Van Brunt, "Stochastic Properties of Negative Corona (Trichel) Pulses in SF₆/O₂ Mixtures", *Proceedings Ninth International Conference on Gas Discharges and Their Applications*, Benetton, Editore, Padova, pp. 227-230, 1988.
- [16] S. V. Kulkarni, R. J. Van Brunt, and V. K. Lakdawala, "Transition from Trichel-Pulse Corona to Dielectric-Barrier Discharge", *Annual Report, 1990 IEEE Conference on Electrical Insulation and Dielectric Phenomena*, Pocono Manor PA, pp. 267-274, 1990.
- [17] R. J. Van Brunt, and E. W. Cernyar, "Influence of Memory Propagation on Phase-Resolved Stochastic Behavior of ac-Generated Partial Discharges", *Appl. Phys. Lett.*, Vol. 58, pp. 2628-2630, 1991.
- [18] D. L. Snyder, *Random Point Processes*, John Wiley and Sons, New York, NY, 1975.
- [19] J. P. Steiner, *Digital Measurement of Partial Discharge*, Ph. D. Thesis, Purdue University, W. Lafayette, IN, May 1988.
- [20] G. W. Trichel, "The Mechanism of the Negative Point to Plane Corona Near Onset", *Phys. Rev.*, Vol. 54, pp. 1078-1084, 1938.
- [21] L. B. Loeb, A. F. Kip, G. G. Hudson, and W. H. Bennett, "Pulses in Negative Point-to-Plane Corona", *Phys. Rev.*, Vol. 60, pp. 714-722, 1941.
- [22] R. Morrow, "Theory of Stepped Pulses in Negative Corona Discharges", *Phys. Rev. A*, Vol. 32, pp. 3821-3824, 1985.
- [23] J. A. Cross, R. Morrow, and G. N. Haddad, "Negative Point-Plane Corona in Oxygen", *J. Phys. D: Appl. Phys.*, Vol. 19, pp. 1007-1017, 1986.
- [24] D. A. Scott and G. N. Haddad, "Negative Corona in Nitrogen-Oxygen Mixtures", *J. Phys. D: Appl. Phys.*, Vol. 20, pp. 1039-1044, 1987.
- [25] W. L. Lama and C. F. Gallo, "Systematic Study of the Electrical Characteristics of the 'Trichel' Current Pulses from Negative Needle-to-Plane Coronas", *J. Appl. Phys.*, Vol. 45, pp. 103-113, 1975.
- [26] J. P. Steiner and F. D. Martzloff, "Partial Discharges in Low-Voltage Cables", *Conference Record of the 1990 IEEE International Symposium on Electrical Insulation*, Toronto Canada, pp. 149-152, 1990.
- [27] M. Beyer, W. Kamm, H. Borsi, and K. Feser, "A New Method for Detection and Location of Distributed Partial Discharges (Cable Faults) in HV Cables Under External Interference", *IEEE Trans. on Power Apparatus and Systems*, Vol. 101, pp. 3431-3438, 1982.
- [28] M. S. Mashikian, R. B. Northrop, Rajcev Bansal, and C. L. Nikias, "Method and Instrumentation for the Detection, Location and Characterization of Partial Discharges and Faults in Electric Power Cables", *U. S. Patent 4887, 041*, Dec. 12, 1989.
- [29] J. P. Steiner and W. L. Weeks, "Digital Estimation of Partial Discharge", 1987 Annual Report, *Conference on Electrical Insulation and Dielectric Phenomena*, Gaithersburg MD, pp. 73-78, 1987.
- [30] K. L. Strickle, E. F. Kelley, H. Yamashita, C. Fenimore, M. O. Pace, T. V. Blalock, A. L. Wintenberg, and I. Alexeff, "Observations of Partial Discharges in Hexanes under High Magnification", *IEEE Trans. on Electr. Insul.*, Vol. 26, pp. 692-698, 1991.
- [31] R. Kattan, A. Denat, and O. Lesaint, "Generation, Growth, and Collapse of Vapor Bubbles in Hydrocarbon Liquids Under a High Divergent Electric Field", *J. Appl. Phys.*, Vol. 66, pp. 4062-4066, 1989.
- [32] H. I. Marsden and P. B. McGrath, "An Optical study of Prebreakdown Events in ac-stressed n-hexane", *IEEE Trans. Electr. Insul.*, Vol. 26, pp. 266-270, 1990.
- [33] E. F. Kelley, M. Nehmadi, R. E. Hebner, M. O. Pace, A. L. Wintenberg, T. V. Blalock, and J. V. Foust, "Measurement of Partial Discharges in Hexane under dc Voltage", *IEEE Trans. Electr. Insul.*, Vol. 24, pp. 1109-1119, 1989.
- [34] M. O. Pace, A. L. Wintenberg, T. V. Blalock, E. F. Kelley, G. J. FitzPatrick, C. Fenimore, and H. Yamashita, "Pressure Effects on Partial Discharges in Hexane under DC Voltage", 1989 Annual Report, *Conference on Electrical Insulation and Dielectric Phenomena*, Leesburg VA, pp. 87-92, 1989.
- [35] P. K. Watson and W. G. Chadband, "The Dynamics of Pre-Breakdown Cavities in Viscous Fluids in Negative Point-Plane Gaps", *IEEE Trans. Electr. Insul.*, Vol. 23, pp. 729-738, 1988.

- [36] E. F. Kelley, "An Image-Preserving Optical Delay for High-Speed Photography", Record of the 42nd Annual Conference of the Society for Imaging Science and Technology, Boston MA, pp. 293-296, 1989.
- [37] A. L. Wintenberg, T. V. Blalock, and M. O. Pace, "High-Bandwidth Measurement of Low-Level Pre-breakdown Currents in Liquid Dielectrics", Conference Record of the 1990 IEEE International Symposium on Electrical Insulation, Toronto Canada, pp. 422-426, 1990.
- [38] T. V. Blalock, A. L. Wintenberg, and M. O. Pace, "Low-noise Wide-band Amplification System for Acquiring Prebreakdown Current Pulses in Liquid Dielectrics", IEEE Trans. Electr. Insul., Vol. 24, pp. 641-647, 1989.
- [39] R. J. Van Brunt, M. Misakian, S. V. Kulkarni, and V. K. Lakdawala, "Influence of a Dielectric Barrier on the Stochastic Behavior of Trichel-Pulse Corona", IEEE Trans. Electr. Insul., Vol. 26, pp. 405-415, 1991.

This paper is based on a presentation given at the 1990 Volta Colloquium on Partial Discharge Measurements, Como, Italy, 4-5 September 1990.

Manuscript was received on 12 April 1991, in revised form 22 July 1991